DOI 10.1007/s11182-022-02527-2
Russian Physics Journal, Vol. 64, No. 10, February, 2022 (Russian Original No. 10, October, 2021)

INVESTIGATION OF THE STRUCTURAL, OPTICAL, AND ELECTRICAL CHARACTERIZATION OF FeO-DOPED ZnO NANOPARTICLES

A. Haj Ismail,[1,2] F. Haj Jneed,[3] and E. A. Dawi[1,2] UDC 539.2

In this work, FeO-*doped* ZnO *nanoparticles (*FeO-ZnO *NPs) were synthesized by the chemical method of sol-gel coating on glass substrates with concentrations of [0%, 3%, and 5%]. The properties of the synthesized* FeO-*doped* ZnO *NPs films were investigated in terms of their structural, optical, and electrical properties. X-ray diffraction (XRD) was used to study the crystal structure, crystal growth, and chemical composition of the samples. The UV-Vis spectra of the synthesized films show a blue shift in the optical bandgap of the* ZnO *nanoparticles integrated with* FeO*. Electrical properties of the* FeO-*doped* ZnO-*NP films were investigated as a function of temperature. A linear relationship between ln(R) and 1/T was found.*

Keywords: FeO, nanoparticles, thin films, ZnO, photocatalysis.

INTRODUCTION

Nanoparticles (NPs) are currently experiencing a wide scientific and technological interest due to their optical, catalytic, and electrical properties and because some of their specific physical properties are different from those of the corresponding bulk material [1-5]. Nowadays, NPs are extensively studied, either in arrays or as single particles in various scientific applications such as improved solar cells [6,7], chemical (bio) sensors [8], medical treatment and diagnostics [9]. Among the available nanomaterials, semiconducting nanoparticles are a large class that have gained much scientific interest due to their useful properties and applications in various fields in biomedicine [10,11] and biology [12,13]. Metal oxide NPs are considered as one of the prominent and most widely used materials due to their diverse characterizations and functionalities. Among the various metal oxide NPs, the zinc oxide (ZnO) shows good activity and stability under irradiation in both acidic and basic atmosphere. However, the pure ZnO shows much lower photocatalytic activity even under UV irradiation due to its wide band gap (3.37 eV) [14]. To improve the photocatalytic activity, it is necessary to couple ZnO with another semiconductor with a lower band gap. Iron oxide (FeO) is a *p*-type semiconductor with a small band gap (2.2 eV) and coupling with ZnO, leads to the formation of heterojunctions. The photo-generated electrons of ZnO readily migrate to FeO, leading to an enhancement of the photocatalytic activity. The physical, optical, and chemical properties of ZnO and FeO make them excellent candidates for use in heterogeneous catalytic applications, sensors, photodetectors, and ultraviolet applications. Moreover, the use of ZnO NPs offers a promising technology for reducing environmental pollution.

The aim of this study is to synthesize FeO-doped ZnO NPs and further analyze their structural, optical, and electrical properties. A detailed overview of the method is given, followed by a discussion of the resulting structural, optical, and electrical properties of the FeO-doped-ZnO NPs samples.

[1]Ajman University, United Arab Emirates, e-mail: a.hajismail@ajman.ac.ae; [2]Nonlinear Dynamics Research Centre NDRC, Ajman University, United Arab Emirates; [3]Department of Physics, University of Aleppo. Translated from Izvestiya Vysshikh Uchebnykh Zavedenii, Fizika, No. 10, pp. 60–65, October, 2021. Original article submitted July 21, 2021.

TABLE 1. Overview of the XRD Parameters and Crystallite Size

	Crystallite size, nm		
Peak	100	002	101
FeO-doped ZnO, 0%	25.81	23.57	26.79
FeO-doped ZnO, 3%	22.37	21.49	24.35
FeO-doped-ZnO, 5%	20.65	19.72	21.13

MATERIALS AND METHODS

The FeO-doped ZnO photocatalysts were prepared by simple co-deposition using sol-gel dip coating technique, which is a simple method that requires considerably less equipment and is widely used in coating technology [15]. Glass substrates were prepared with a size of 5 x 2.5 cm^2 and then, cleaned with hydrochloric acid (HCI, concentration of 5%) in a water bath for 30 minutes. Occasionally, the samples were cleaned with distilled water and ethanol (99% purity) before drying with hydrogen flow. For precipitation, zinc chloride ($ZnCl_2$, 99%) was mixed with ferric chloride ($FeCl_3$) (at 0%, 0.03%, and 0.05%) in highly purified distilled water and mixed with a magnetic mixer for 2 hours to achieve complete solubility. The glass substrates were placed on a heater and the temperature was gradually increased from 300K to 500K. To obtain a good thickness of the prepared thin films, three rounds of the coating process were carried out. Finally, the thin films were gradually cooled and then, annealed at 800K for an annealing time of 2 hours.

RESULTS AND DISCUSSION

Structural Properties

An X-Ray diffraction system (XRD) was used to analyze the structural characteristics of the FeO-doped-ZnO samples. The XRD uses a copper cathode with a wavelength of $\lambda = 1.54178$ Å, a current of 0.1 mA, a voltage of 35 kV, and a rotation angle of 2θ in the range 20–80° and with a shift of 0.1^o every 10 s. Figure 1 shows that the incorporation of FeO into the ZnO ions results in a notable decrease in the relative intensity of all XRD peaks. Besides, XRD peaks indicate broadening at half maximum with increasing FeO doping percentage in the ZnO films. The estimation of the crystallite size *D* can be obtained from the Scherrer equation [8]:

$$D = \frac{K\lambda}{\beta\cos(\theta)}, \tag{1}$$

where $K = 0.94$ is the Scherrer constant, λ is the wavelength of the radiation, β is the width at the half-peak-height of an XRD line, and θ is the diffraction angle. XRD results are presented in Table 1.

Optical Properties

A UV device (WIN5-SPERTROPHOTO METER) was used to analyze the optical properties of the prepared ZnO thin films. The spectrum of FeO-doped ZnO NPs is studied in a wavelength range of 300-800 nm and presented in Fig. 2. A peak shift is observed in the presented spectra, which corresponds to the presence of both ZnO and FeO. Also, an increase in the thickness of the thin film results in a change in the height of the peak, following the Ampere's low:

$$I = I_0 \exp^{-\alpha x}, \tag{2}$$

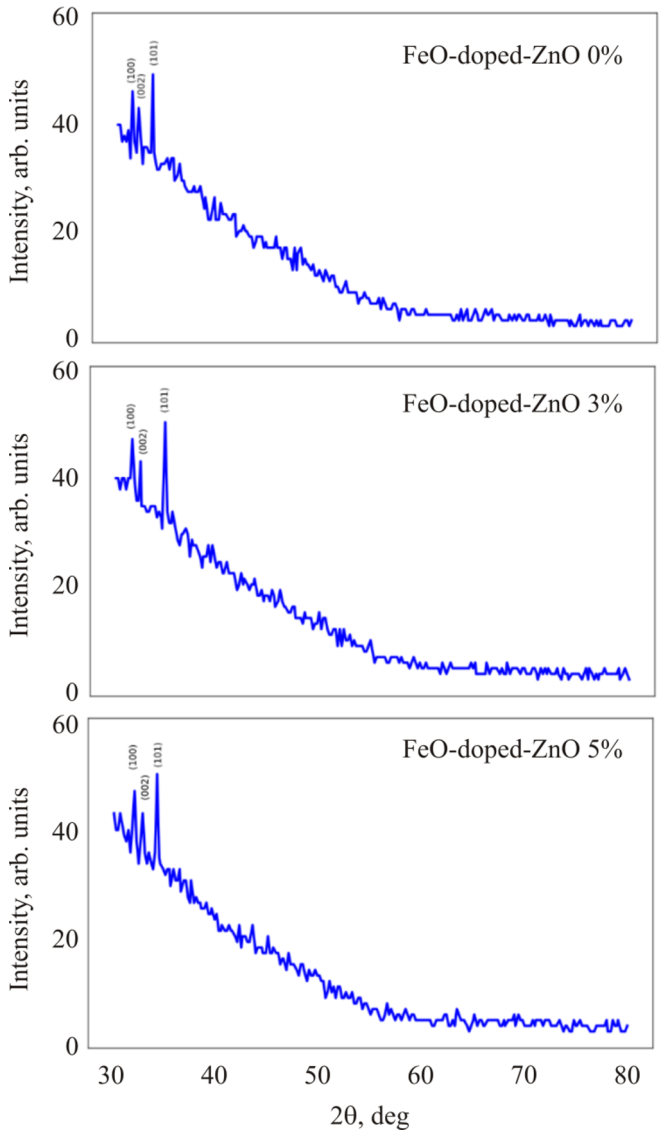

Fig. 1. X-Ray diffraction (XRD) pattern of FeO-doped ZnO nanoparticles.

where I is the light intensity on the film, I_0 is the intensity of the incident light, and α is the absorption coefficient. As can be seen, a decrease in the absorbance is observed, which is correlated to indirect transitions between the valence and conduction bands according to the Lucy equation:

$$\alpha h\nu = B(h\nu - E_g)^2 . \quad (3)$$

Here, α is the absorption coefficient, $h\nu$ is the energy of the incident photon, E_g is the energy band, and B is a constant given as:

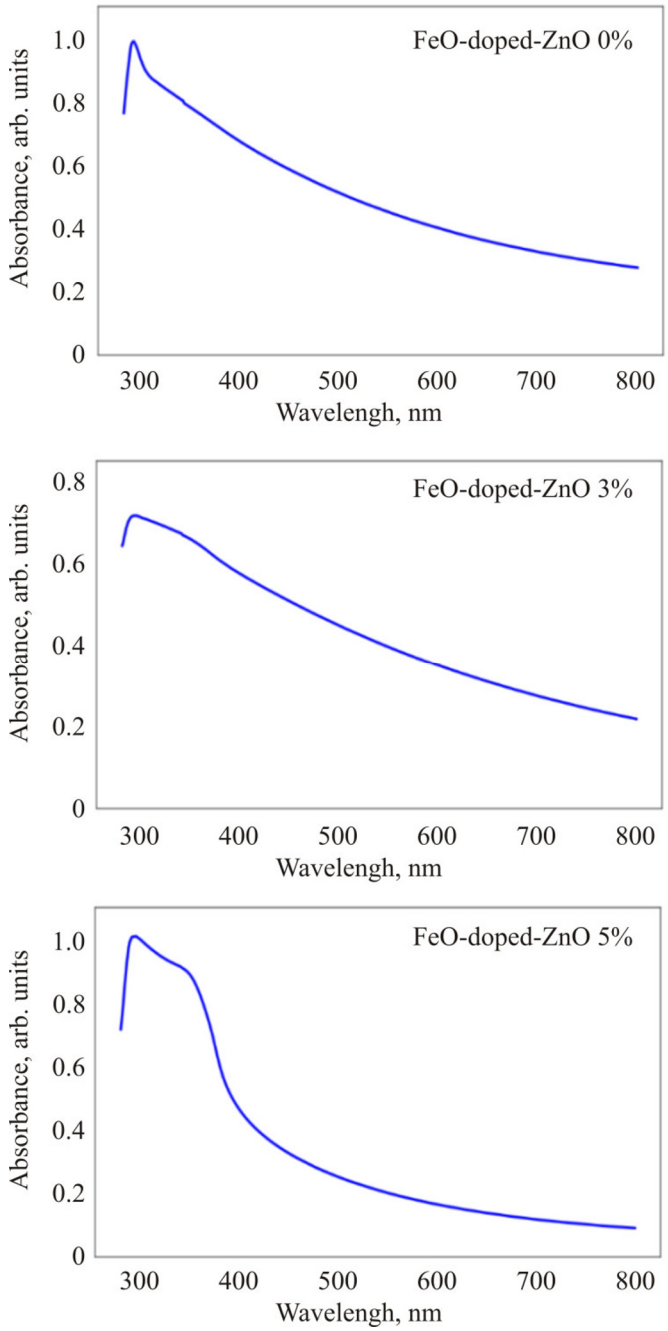

Fig. 2. Spectra of the prepared thin films deposited on glass substrates.

$$B = \frac{4\pi\sigma_0}{ncE_0}, \tag{4}$$

where E_0 is the initial energy, n is the refraction index, and σ_0 is the electrical conductivity at an absolute zero temperature. Furthermore, the energy gap was obtained using the following equation:

TABLE 2. The Energy Gap of Prepared Thin Films

Sample	E_g
FeO-doped ZnO 0%	3.14
FeO-doped ZnO 3%	2.90
FeO-doped ZnO 5%	2.72

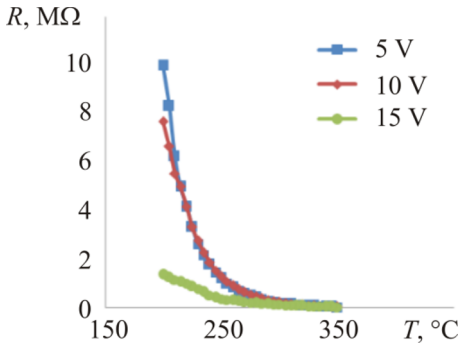

Fig. 3. The resistance as a function of temperature of FeO-ZnO (5%) thin films at three different electrical potentials (5 V, 10 V, and 15 V).

$$E_g = \frac{\alpha h\nu - (\alpha h\nu)^2}{\alpha}. \tag{5}$$

The energy gap of the prepared thin films is presented in Table 2. The energy gap is observed to be maximum for pure thin films. However, with decreasing the purity of the sample, the energy gap is found to decrease.

Electrical properties

The temperature dependence of electrical conductivity of the FeO-doped ZnO thin films was analyzed using the following equation:

$$\rho = \rho_0 \exp^{\beta/T}, \tag{6}$$

where ρ is the resistivity, T is the temperature, and $\beta = E_a / 2KT$.

To discuss the electrical conductivity, we investigated the relationship between the resistivity and temperature for FeO-ZnO (5%) thin films at three different electrical potentials of (5 V, 10 V, and 15 V) as shown in Fig. 3. It shows that as the temperature increases, the resistivity of the films decreases for the whole range of the selected voltages. Figure 4 shows the relationship between the resistance and the inverse temperature for three selected voltages (5 V, 10 V, and 15 V). A linear relationship between ln(R) and 1/T can be seen. The activation energy for different electric potentials can be obtained from the slope of ln(R) and 1/T, which is shown in Table 3.

TABLE 3. Activation Energy and β at Different Electrical Potentials

V, V	5	10	15
β	10875	10745	10305
E_a	0.8831	0.8567	0.8393

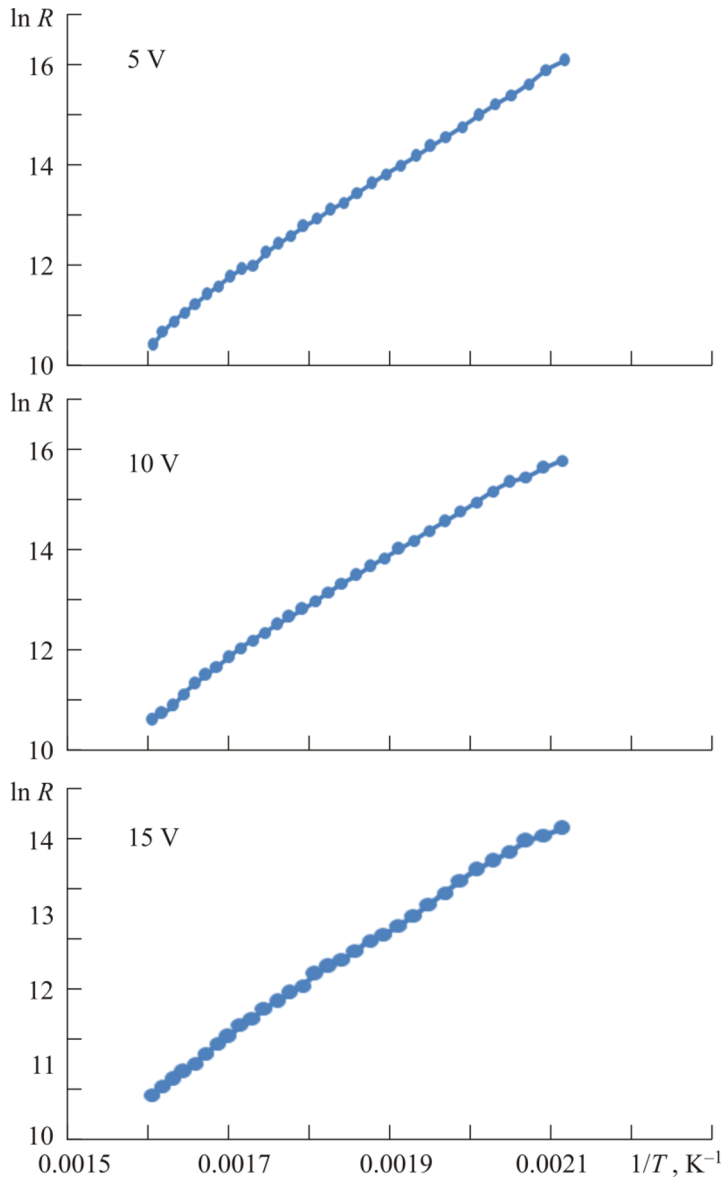

Fig. 4. The relation between *ln(R)* and *1/T* of FeO-ZnO (5%) thin films at three different electrical potentials (5 V, 10 V, and 15 V).

CONCLUSIONS

We have investigated the properties of thin films of FeO-doped ZnO (with the concentrations of [0%, 3%, and 5%]). The analysis of the structural properties corresponding to the crystalline dimensions of the thin films confirmed a nanostructure in the prepared thin films. Moreover, the absorption spectrum of the thin films shows that an increase in the percentage of FeO used leads to an increase in the width of the peak of the absorption spectrum. Furthermore, it was found that there is a linear relationship between $\ln(R)$ and $1/T$. Finally, the activation energy at different differential potentials was investigated and a decrease in activation energy with increasing voltage was observed.

Funding Statement: The authors received no specific funding for this study.

Conflicts of Interest: The authors declare that they have no conflicts of interest to report regarding the present study.

REFERENCES

1. J. M. Gerardy and M. Ausloos, Phys. Rev. B, **25**, 4204 (1982).
2. J. J. Penninkhof, A. Polman, L. A. Sweatlock, A. M. Stefan, A. Harry, A. Vredenberg, and B. J. Kooi, Applied Physics Letters, **83**, 4137 (2003).
3. T. W. Ebbesen, H. J. Lezec, H. F. Ghaemi, T. Thio, and P. A. Wolff, Nature, **391**, 667 (1998).
4. R. Elghanian, J. Storhoff, R. C. Mucic, R. L. Letsinger, and C. A. Mirkin, Science, **277**, 1078 (1997).
5. R. P. Cowburn, Journal of Physics D: Applied Physics, **33**, R1 (2000).
6. K. R. Catchpole and S. Pillai, Journal of Luminescence, **121**, 315 (2006).
7. K. Seok-Soon, N. Seok-In, J. Jang, K. Dong-Yu, and N. Yoon-Chae, Applied Physics Letters, **93**, 073307(2008).
8. J. H. Amanda, S. Zou, G. C. Schatz, and R. P. Van Duyne, The Journal of Physical Chemistry B, **108**, 6961 (2004).
9. L. A. Bauer, N. S. Birenbaum, and J. G. Meyer, Journal of Materials Chemistry, **14**, 517 (2004).
10. J. Jinhuan, P. Jiang, C. Jiye, **2018**, 1 (2018).
11. P. K. Mishra, H. Mishra, A. Ekielski, S. Talegaonkar, and B. Vaidya, Drug Discovery Today, **22**, 182 (2017).
12. M. Y. Hidayat, M. Rosfarizan, Z. Uswatun, and A. N. Aini, Journal of Animal Science and Biotechnology, **57** (2019).
13. S. Neha, S. Manish, P. K. Mishra, and R. Pramod, Frontiers in Microbiology, **7**, 514 (2016).
14. L. J. Chebor, International Journal of Scientific Engineering and Science, **2**(2), 5-8 (2018).
15. S. Prasad, V. Kumar, S. Kirubanandam, and A. Barhoum, Emerging Applications of Nanoparticles and Architecture Nanostructures, 305 (2018).
16. A. S. Edelstein, Encyclopedia of Materials: Science and Technology (2001).